ADVANCED THERAPEUTICS
www.advtherap.com

Study on Significance of Receptor Targeting in Killing of Intracellular Bacteria with Membrane-Impermeable Antibiotics

Rosa Catania, Francesca Mastrotto, Chris J. Moore, Cynthia Bosquillon, Franco H. Falcone, Alan Huett, Giuseppe Mantovani, and Snow Stolnik**

Water-soluble antibiotics are largely excluded from therapy of intracellular infections, such as *Shigella* spp., *Listeria* spp., or *Salmonella* spp., due to their inability to permeate mammalian cell membrane. Here, the authors study if targeting offers an advantage to deliver killing doses of membrane-impermeable antibiotics intracellularly to infected cells. Mannose-decorated liposomes, loaded with gentamicin, are fabricated to target mannose receptor, a recognition system of (infected) macrophages. Designing a family of liposomes with varying surface presentation of mannose ligand, the authors show a clear dependence of cellular internalization on the ligand surface presentation. Significantly for the killing of intracellular bacteria, the study demonstrates internalization of mannosylated liposomes by the entire population of macrophages, both *Salmonella*-infected and non-infected, resulting in an efficient treatment of intracellular infection. This contrasts with non-targeted liposomes, where internalization does not occur by a substantial subpopulation of infected cells. The study points to the significance of targeted delivery of antibiotics for treatment of intracellular infections.

1. Introduction

It is crucial for the successful resolution of intracellular infections to deliver killing doses of antibiotic intracellularly to infected cells to both eradicate infection and reduce the risk of antimicrobial resistance associated with subtherapeutic doses. These intracellular infections include major pathogens such as *Shigella* spp., *Listeria* spp., or *Salmonella* spp. *Salmonella* infections alone are responsible for 16 million cases of typhoid fever, 94 million cases of gastroenteritis, and 600000 deaths each year[1]—many complicated by antimicrobial resistance.[2] Therefore, to reduce the risk of widespread resistance acquisition, it is of paramount importance that effective doses of antibiotics are delivered and present intracellularly. However, water-soluble antibacterial agents are largely excluded from therapy of intracellular infections due to their cell membrane-impermeability and consequent lack of exposure.

Particulate nano-carriers, such as polymeric or lipid-based nanoparticles, liposomes, and micellar or emulsion systems, are extensively researched and utilized to overcome limitations of drug molecules, including low solubility, bioavailability, pharmacokinetics, or toxicity, as well as poor permeability across biological barriers and membranes. Amongst the nano-carriers, liposomes research resulted in a number of formulations reaching clinic, including a few examples of liposomal products for antibiotics; example, AmBiosome and MiKasome.[3] These "classical" formulations demonstrate that encapsulation of antibiotics into liposomes reduces their toxic side-effects to the host due to improved pharmacokinetics. Studies furthermore show that encapsulation into liposomes of membrane-impermeable antibiotics (gentamicin) improves its intracellular delivery and results in appreciable antibacterial activity.[4] In a further technology advancement, and studied here, a concept of targeting by surface functionalization of a nano-carrier, widely adopted in a design of nano-carriers for application in cancer, has been suggested.[5] Targeted antibacterial formulations have the potential to overcome limitations of current antibiotic therapies, which make little distinction between body sites, resulting in selection for resistance in the patient microbiota, which becomes a source of resistance genes[6] and further infection.[7] Targeted antibiotics delivery could reduce collateral disruption of the patient microbiome. Antibiotic-associated loss of microbiome-mediated

R. Catania, C. Bosquillon, F. H. Falcone, G. Mantovani, S. Stolnik
Division of Molecular Therapeutics and Formulation, School of Pharmacy
University of Nottingham
Nottingham NG7 2RD, UK
E-mail: giuseppe.mantovani@nottingham.ac.uk;
snjezana.stolnik@nottingham.ac.uk
R. Catania, C. J. Moore, A. Huett
School of Life Sciences
University of Nottingham
Queens Medical Centre, Nottingham NG7 2UH, UK
F. Mastrotto
Department of Pharmaceutical and Pharmacological Sciences
University of Padova
Padova 35131, Italy

The ORCID identification number(s) for the author(s) of this article can be found under https://doi.org/10.1002/adtp.202100168

DOI: 10.1002/adtp.202100168

infection resistance has been identified as a key contributor to nosocomial and antibiotic-related infection, as niche occupancy and direct bacteria–bacteria competition form a major barrier to colonization and infection by pathogenic strains.[8,9]

In this context, our study investigates the significance of targeting liposomes to infected cells to deliver intracellularly a membrane-impermeable antibiotic (gentamicin), otherwise not effective in therapy of intracellular infections. We exploit mannose receptor (CD206) expressed on the macrophages plasma membrane to achieve receptor-driven internalization of mannosylated liposomes, and their antibiotic cargo, to *Salmonella*-infected macrophages.

Targeting of overexpressed mannose receptor is explored as a strategy in cancer therapy to target tumor-associated macrophages.[10–12] Regarding targeting macrophages for treatment of intercellular bacterial infections this has not as yet been addressed adequately, as reviewed by the Schlesinger's group.[13] Recent studies exploit mannose either as a ligand which is chemically conjugated with antibiotic ciprofloxacin in a treatment of pneumonic tularemia,[14] to synthesize mannose-functionalized polymers which show intracellular bactericidal activity,[15] or as mannose-based synthetic polymers which were proposed to "anchor" at biofilms and in that way achieve localized antibiotics delivery,[16] and achieve all approaches and technologies fundamentally different to the current study. In another approach, mannose-surface conjugated and cross-linked polymeric nanogel was designed to achieve in vitro internalization and antibiotic delivery to macrophages.[17] An increased efficacy was observed for the macrophages treated with nano-gel against *Staphylococcus aureus* (*S. aureus*) infection. However, experiments were not conducted to provide a mechanistic understanding that underpins the observed difference—which is the focus of the present study.

It should be appreciated that for efficient engagement with mannose receptor a ligand multivalency is considered essential;[18] this property is a hallmark of carbohydrate–carbohydrate receptor interactions.[19–22] Multivalency can be achieved in different ways: by spatial proximity of contiguous individual sugar ligands presented at the liposome surface or by presentation of a cluster of ligands where individual ligands are "preclustered" by a macromolecular structure. Here, we exploit mannose ligand presentation as multiple copies of either individual monovalent or oligo-valent ligands, the latter containing mannose residues as pendent units of an oligomeric chain. We employed a new strategy for rapid synthesis of defined oligo-mannose ligands via controlled radical polymerization to synthesize a family of membrane-inserting glycolipid ligands and used these to fabricate a library of liposomes with varying presentations of mannose surface glycosylation in order to study the importance of targeted antibiotics delivery to infected cells.

2. Results

2.1. Membrane-Inserting Mannose Ligands Synthesis and Characterization

To formulate liposomes capable of macrophages-targeting, that is, interacting with binding domains of the mannose (CD206) receptor, we synthesized a set of lipid bilayer inserting mannose glycolipids: the monovalent Chol-Man1 and the oligo-valent Chol-Man10 and Chol-Man20 (**Figure 1**). Cholesterol was selected as the inserting ("anchor") moiety, as previously shown to efficiently insert within phospholipids bilayers.[23–26]

First, compound 1 (Figure 1 and Figures S1–S3, Supporting Information) was synthesized by reacting commercially available cholesteryl chloroformate with 2-(2-aminoethoxy) ethanol. Mannosylated cholesterol Chol-Man_1, compound 4 (Figure 1 and Figures S9–S11, Supporting Information), was then prepared by Koenigs–Knorr reaction, using 2,3,4,6-tetra-*O*-acetyl-D-mannopyranosyl iodide 2 (Figure 1 and Figures S4 and S5, Supporting Information), synthesized in two steps from mannose pentaacetate (Scheme S1, Supporting Information), as the glycosyl donor. Deacetylation of the tetraacetate mannosylated cholesterol compound 3 (Figure 1 and Figures S6–S8, Supporting Information) with K_2CO_3 in CH_3OH, then afforded the final Chol-Man_1. Short cholesterol-terminated mannose oligomers containing 10 or 20 mannose units (DP 10 and 20) were synthesized following an adapted version of Perrier's ultrafast reversible addition fragmentation chain transfer (RAFT) polymerization,[27] using 2′-acrylamidoethyl-α-D-mannopyranoside 12 (Figure 1 and Scheme S2 and Figures S21–S25, Supporting Information) as the monomer, and cholesterol-containing chain-transfer agent (CTA) 6. Cholesterol is a hydrophobic molecule with very low water solubility, while RAFT polymerization of sugar monomers is typically carried out under aqueous conditions, making it challenging to find polymerization conditions where all components—monomer, CTA and radical initiator—were soluble, even in the presence of organic cosolvents. We reasoned that this issue could be overcome by carrying out the polymerization under biphasic organic–water conditions using an amphiphilic CTA able to orient itself at the solvent interphase, with cholesterol located in the organic hydrophobic phase and the polar trithiocarbonate CTA head pointing toward the water phase, where it could mediate the RAFT polymerization process and afford the required cholesterol-terminated oligomeric ligands. Accordingly, we designed the amphiphilic cholesterol CTA, compound 6, which was prepared by reacting the cholesteryl alcohol 1 with 2-bromo-propionyl bromide and Et_3N to give the bromoester 5 (Figure 1 and Figures S12–S14, Supporting Information), which was treated with trithiocarbonylpropane sulfonate sodium salt 11 (Figure 1 and Figures S15–S17, Supporting Information) in the presence of 15-crown-5 crown in acetone, to give the cholesterol CTA product 6 (Figure 1 and Figures S18–S20, Supporting Information). Finally, ultrafast RAFT polymerization, carried out under biphasic conditions (water/toluene) at 100 °C for 20 min, followed by precipitation in THF and treatment with an excess of 4,4′-azobis(4-cyanovaleric acid) at 90 °C to remove the trithiocarbonate chain-end functionality,[28] afforded the cholesterol-terminated ligands Chol-Man_{10} and Chol-Man_{20} (Figure 1 and Figures S26–S30, Supporting Information).

2.2. Mannose-Modified Liposomes: Biophysical Characterization

To define a design space for surface glycosylation of liposomes capable of engaging with CD206, and achieving receptor-mediated endocytosis, we fabricated a set of liposomes (Table S1 and Figure S35, Supporting Information) with varying surface displays

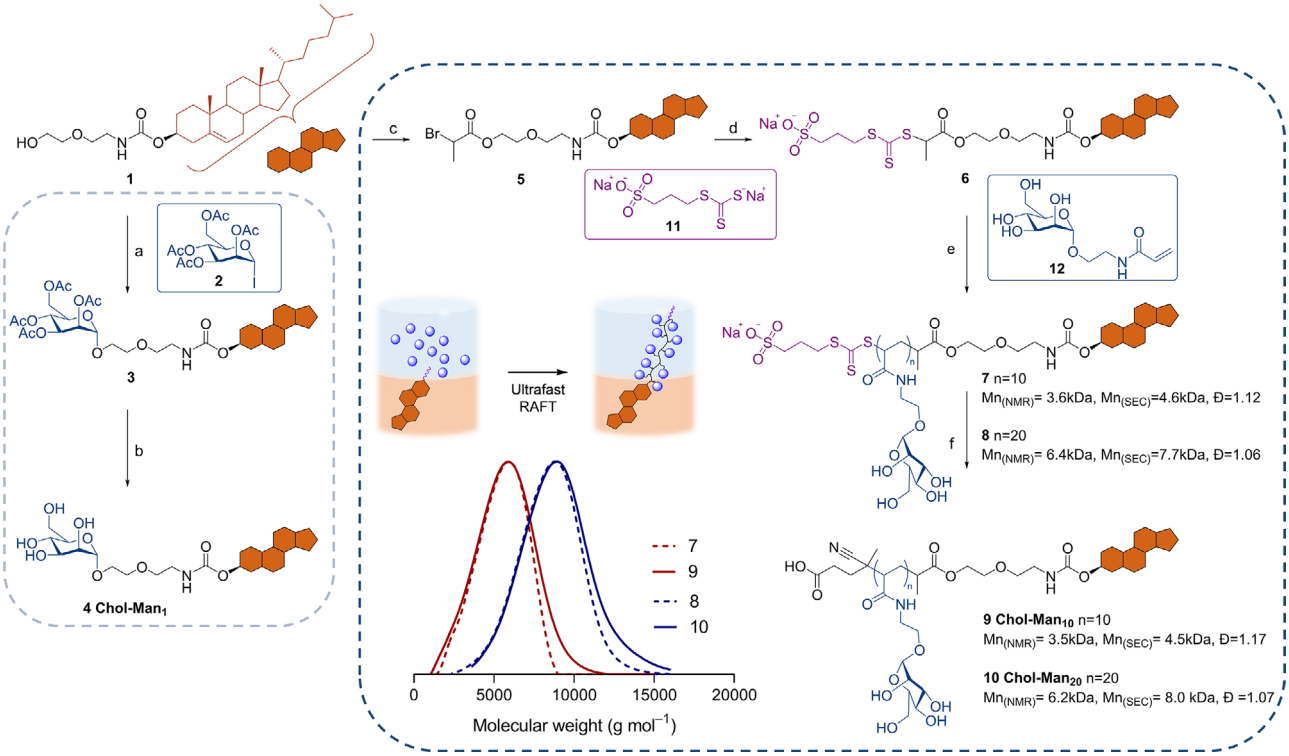

Figure 1. Synthesis of cholesterol-containing monovalent, Chol-Man_1, and oligo-valent glycolipid ligands Chol-Man_{10} and Chol-Man_{20}. Reagents and Conditions: a) Ag_2CO_3, anhydrous CH_2Cl_2; b) K_2CO_3, CH_3OH; c) 2-bromo propionyl bromide, CH_2Cl_2, Et_3N, 0–25 °C; d) 15-crown-5; acetone; e) VA-044, H_2O, toluene, 100 °C, 20 min; f) V-501, DMSO, 90 °C, 75 min. Insert: SEC analysis of cholesterol-mannose oligomers before and after removal of the trithiocarbonate end-group (mobile phase: DMF + 0.1% LiBr).

of mannose ligand, in terms of content and spatial distribution of the ligands at the surface, as illustrated in **Figure 2**A.

All fabricated liposomes have an average hydrodynamic diameter between 110 and 170 nm (Figure 2B), that is, within the size appropriate for clathrin-mediated endocytosis driven by mannose receptor,[29,30] and show good colloidal stability in a suspension. We initially assessed glycosylated liposomes' ability to engage with the targeted receptor in in vitro conditions by measuring aggregation of liposomes on addition of a model mannose-binding lectin, concanavalin A (ConA);[31–34] the experimental set up that eliminates potential non-specific interactions of the liposomes that could occur in more complex conditions including cells. The resulting kinetic rates of lectin-mediated aggregation (agglutination) in Figure 2C (and Figure S36A,B, Supporting Information) allow different cross-comparisons to be made on liposome formulations designed (as grouped in Figure 2). These comparisons, in summary, illustrate that surface presentation of mannose as mono-ligand fails to initiate aggregation of such modified liposomes (L-(Chol-Man_1)$_{10\%}$), and that a "lower limit" of surface mannosylation to achieve receptor engagement may be with oligo-ligand in L-(Chol-Man_{10})$_{1\%}$ liposomes, whilst an "upper limit" may lie between L-(Chol-Man_{10})$_{10\%}$ and L-(Chol-Man_{20})$_{10\%}$ formulations containing 10 mol% of oligo-mannose ligands. Comparing surfaces with (statistically) higher density of shorter oligo-ligands, for example, in L-(Chol-Man_{10})$_{10\%}$ and lower density of longer oligo-ligands, in, for example, L-(Chol-Man_{20})$_{5\%}$, points to the prominence of surface density. This is further illustrated in the aggregation propensity of L-(Chol-Man_{20})$_{0.5\%}$ < L-(Chol-Man_{20})$_{5\%}$ < L-(Chol-Man_{20})$_{10\%}$. Taken together, the ConA aggregation screening data demonstrate the importance of the spatial configuration of surface glycosylation, with an interplay between surface ligand density and length to achieve engagement with the model receptor.

2.3. In Vitro Cellular Internalization of Liposomes by Macrophages

Cellular internalization of mannosylated liposomes was assessed in vitro in culture of RAW 264.7 murine macrophages. These cells have previously been used in studies on intracellular infections by *Listeria monocytogenes*,[35] *S. aureus*,[36] and *Salmonella*.[37,38] They express CD206 at rest (unlike other commonly used cell lines of human macrophages such as U937, THP-1, Mono-Mac, and HL60),[39] and expression is increased by treatment with IL-4.[40,41] CD206 is an effective internalization receptor, shown to drive clathrin-mediated endocytosis of an associated ligand,[42] and there is constitutive recycling of the receptor between a membrane-exposed and larger, intracellular pool.[43] The latter means that the majority of CD206 is only accessible to antibody immunostaining following cell permeabilization, as demonstrated in **Figure 3**A and example flow cytometry dot plots in Figure S39, Supporting Information. Literature suggests that *Salmonella* Typhimurium actively modulates macrophage phenotype preferentially toward an M2-like state, and that these macrophages provide a permissive

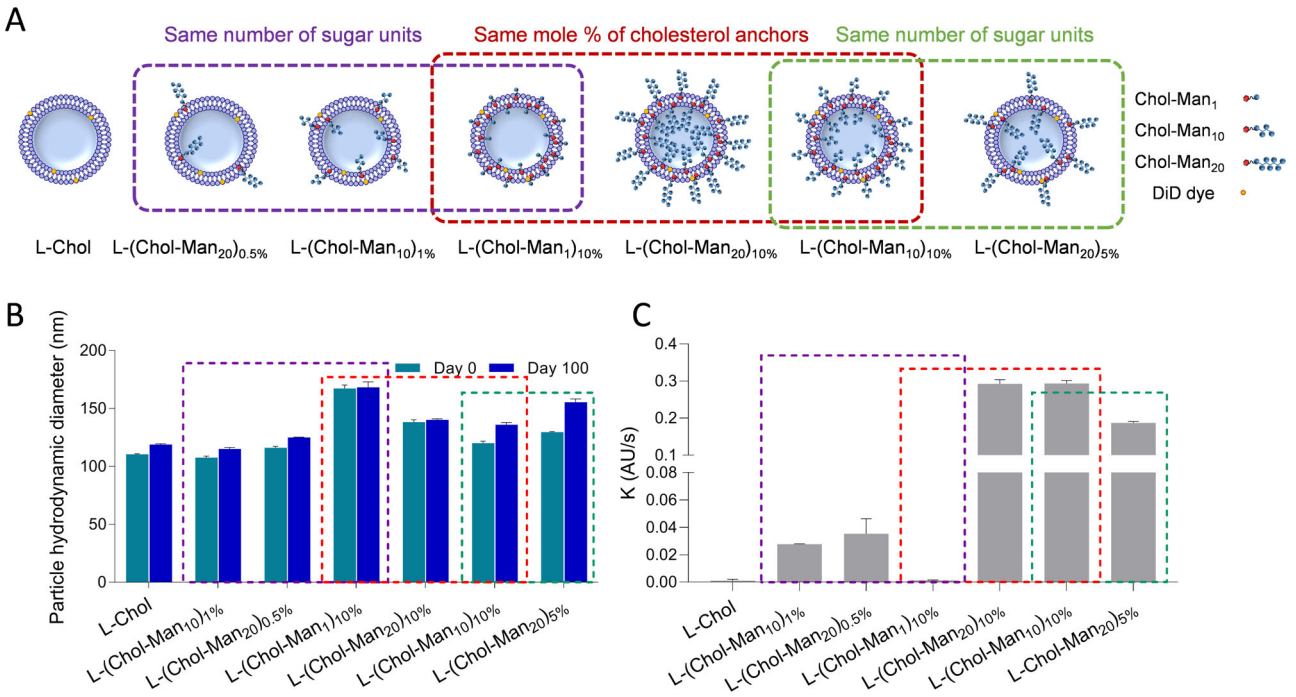

Figure 2. Liposomes composition and biophysical characterization. A) Schematic representation of mannosylated liposomes investigated in this work; "L" denotes liposomes, "Chol-Man" denotes mannose ligands with different number of mannose units: Man_1, Man_{10}, and Man_{20}, for 1, 10, and 20 units; $(Chol\text{-}Man)_{1\%}$, $(Chol\text{-}Man)_{5\%}$, and $(Chol\text{-}Man)_{10\%}$ indicate mol% of cholesterol-containing glycolipid anchor in the liposomal total lipid. Color outlined boxes group liposomal formulations containing equal mol% of cholesterol inserting glycolipid (red), or equal total number of mannose units in varying arrangements (purple for lower, and green for higher mannose content). B) Hydrodynamic average diameter of liposome formulations obtained from dynamic light scattering measurements immediately following fabrication ("Day 0") and after 100 days of storage ("Day 100"). C) Rate of concanavalin A-mediated aggregation of liposome formulations from turbidimetry experiments (K is expressed in arbitrary units/second, AU s^{-1}), calculated via regression of the first 30 s of the aggregation curve (Figure S36A, Supporting Information).

long-term growth infection environment.[44] Therefore, it is likely that M2-like macrophages represent those most in need of intracellular antibiotic delivery to combat *Salmonella* infection. In our study, IL-4-treated RAW 264.7 cells were used as a model to test delivery of membrane-impermeable gentamicin to intracellular *Salmonella* infection, and IL-4 has been shown as a factor in M2 macrophages polarization.[40,45]

Our data initially demonstrate that IL-4 treatment of RAW 264.7 macrophages increases both total as well as surface level of CD206 receptor available for ligand engagement (Figure 3A and Figure S39, Supporting Information), as documented previously.[40,41] Importantly for the proposed mannose receptor-targeted delivery approach, *Salmonella*-infected RAW cells maintained CD206 surface expression levels at the time-point when liposomes treatment was introduced at 2 h following infection (Figure 3A).

Figure 3B summarizes cellular internalization of mannosylated liposomes by RAW 264.7 macrophages under different experimental conditions. Considering formulations in the purple grouping, internalization of L-$(Chol\text{-}Man_1)_{10\%}$ is not statistically significantly different to control non-targeted L-Chol liposomes. This would indicate that cholesterol-based anchoring of a mannose mono-ligand within the liposomal membrane may make the ligand inaccessible for receptor binding, or that the binding, if it occurs, with individual mono-mannose ligands does not result in reorganization of ligands at the liposomal surface, which would create multivalent mannose interaction with sufficient binding avidity to initiate ConA aggregation (Figure 2C) or drive receptor-mediated cellular internalization of such liposomes (Figure 3B). Liposomes bearing L-$(Chol\text{-}Man_{10})_{1\%}$ and L-$(Chol\text{-}Man_{20})_{0.5\%}$ oligo-ligands show low cellular internalization, in agreement with ConA screening in Figure 2C.

It should be remarked here that chemistry of both the membrane anchoring moiety and mannose ligand attachment to the anchor needs to be considered in drawing the above hypotheses. A further experiment, using liposomes surface modified with a mono-mannose ligand attached to a different anchor moiety, palmitoyl, and via tetraethylene glycol "spacer" (compound 14, Scheme S3 and Figures S31–S34, Supporting Information) shows, albeit relatively low, ConA induced aggregation of L-$(Palm\text{-}Man_1)_{10\%}$ liposomes (Figure S37A,B, Supporting Information). The "spacer strategy" is normally employed to increase targeting ligand accessibility to the receptor, typically using ethylene oxide chain as a spacer between anchoring and ligand moieties.[46,47] In our study, Chol-Man_n oligo-ligands in effect provide a "spacer" functionality for $n = 10$ and 20 mannose units (Figure 1), while presenting mannose as "preclustered" multivalent ligand distributed at a certain density at the liposomal surface. The surface presence of mannose oligo-ligands increases the statistical probability for Chol-Man_{10} and Chol-Man_{20} to "instantly" occupy multiple C-type lectin domains of mannose receptor at the cell surface[30]—not requiring the surface

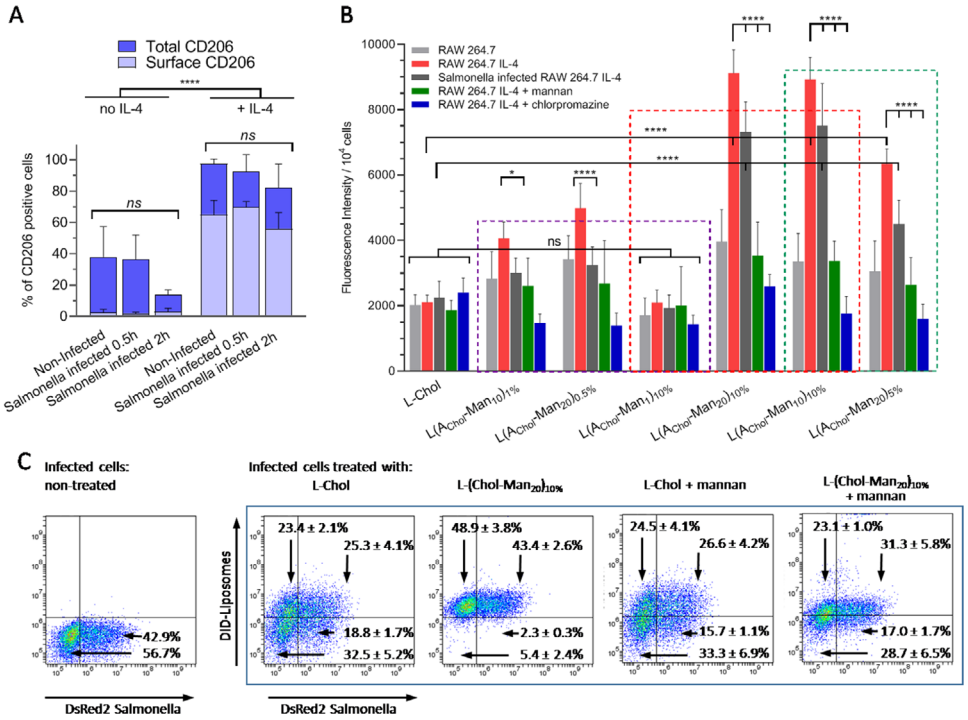

Figure 3. Receptor expression and in vitro cellular internalization of liposomes by macrophages. A) CD206 receptor expression in RAW 264.7 murine macrophages; data shown as percentage of CD206 positive cells. Cells not infected with *Salmonella* Typhimurium SL1344 are denoted as "Non-Infected," and *Salmonella*-infected cells denoted as "Infected 0.5 h" for measurements at 30 min after infection, and "Infected 2 h" for measurements after 2 h. CD206 analysis at 2 h was performed to assess a level of receptor expression at the time point in the infection experiment when liposomes were applied. "Surface CD206" denotes CD206 immunostaining of intact cells, and "Total CD206" of cells permeabilized prior to immunostaining. B) In vitro cellular internalization of liposomes by RAW 264.7 cells under different experimental conditions (cells with no IL-4 treatment, IL-4-treated, IL-4-treated and *Salmonella*-infected, IL-4-treated cells pre-incubated with mannan—CD206 receptor competitor—and IL-4-treated cells pre-incubated with chlorpromazine—clathrin pathway inhibitor). RAW 264.7 cells were incubated with 1 mM of liposomes (total lipids) for 2 h at 37 °C. Formulations tested are grouped as in Figure 2. Selected statistical comparisons annotated in the graph, $^{****}p < 0.0001$, $^{*}p < 0.05$ by two-way ANOVA test; "ns" not statistically different. C) Liposomes' internalization by *Salmonella*-infected RAW 264.7 cells following application of DiD-labeled: control liposomes, L-Chol, or mannosylated liposomes, L-(Chol-Man_{20})$_{10\%}$, under different experimental conditions. Typical dot-plots are shown with the percentages of fluorescent cells indicated within the plots.

clustering of mono-ligands. This is an important consideration in this study, since we fabricated liposomes from a mixture of phospholipids, cholesterol, and sphingomyelin; such a composition increases liposomes stability in biological environment,[48] but would be expected to lead to a formation of liquid organized and disorganized domains within the liposomal lipid bilayer.[49–51] The presence of such domains could lead to a preferential incorporation of glycolipid's inserting moiety into a certain domain, and consequent surface ligand patterning, as well as affecting the inserted glycolipid's ability for lateral diffusion within liposomal membrane and hence tendency for ligand clustering.

Figure 3B data for the purple group liposomes indicate that oligo-ligands in L-(Chol-Man_{10})$_{1\%}$ and L-(Chol-Man_{20})$_{0.5\%}$ are capable of receptor engagement, but that their low density at the surface results in a low probability of lectin aggregation (Figure 2C), as well as interaction with internalizing CD206 receptor. The mannosylated liposomes in the red and green groups follow the general trend seen in ConA aggregation (Figure 2C); they show ≈4.5-fold increase in cellular internalization for L-(Chol-Man_{10})$_{10\%}$ and L-(Chol-Man_{20})$_{10\%}$, and ≈3-fold for L-(Chol-Man_{20})$_5$, relative to non-mannosylated L-Chol liposome counterparts.

Application of mannan, as a competitive ligand for CD206 receptor-driven endocytosis,[52] and chlorpromazine, as inhibitor of clathrin-mediated endocytosis[53,54] implicated in mannose receptor-driven endocytosis, both show statistically significant reduction in cellular internalization of mannose-presenting liposomes. These experiments clearly point to involvement of CD206 receptor-mediated pathway employing clathrin-coated pits in the internalization of mannosylated liposomes (Figure 3B). There is no significant effect of mannan or chlorpromazine on the internalization of non-mannosylated L-Chol liposomes, indicating role of other cellular entry pathways in their internalization. It should be noted here that L-Chol liposomes used in this study as comparative "negative" control were not sterically stabilized by surface modification with, for instance, polyethylene oxide chains ("pegylated"), to minimize their interactions with, and cellular internalization by, the macrophages.[33,55,56]

Focusing on cellular internalization of mannosylated liposomes by *Salmonella*-infected macrophages, this is statistically significantly lower in infected, relative to non-infected cells. However, the values for L-(Chol-Man_{10})$_{10\%}$ and L-(Chol-Man_{20})$_{10\%}$ internalization by infected cells are still approximately fourfold higher than for internalization of non-targeted L-Chol liposomes.

Important for this study are flow cytometry dot-plots in Figure 3C, which provide further details to delineate cellular internalization of mannosylated and non-mannosylated liposomes by non- or *Salmonella*-infected cells. Dot-plot for control, infected but untreated cells ("Infected") reveals that infection of RAW 264.7 macrophages by *Salmonella* is not homogeneous throughout the cell population, with subpopulations of infected and non-infected macrophages present. This heterogeneity in *Salmonella* infection observed in this study is in line with previously documented findings.[57] Crucially for the focus of this study on addressing the importance of targeted delivery, flow cytometry dot-plots (Figure 3C) illustrate that internalization of oligo-mannose presenting L-(Chol-Man_{20})$_{10\%}$ liposomes occurs across the entire cell population, that is, non- and infected cells all show liposomes-associated DiD fluorescence. This is in contrast to non-mannosylated L-Chol liposomes where a substantial subpopulation of infected cells does not show DiD-liposomes uptake; ≈42% of infected (≈19% of total) cell population shows DsRed2 *Salmonella* fluorescence indicating infection, but no DiD fluorescence indicative of liposomes' internalization by these infected cells. Additionally, a comparison of dot-plots for L-Chol and L-(Chol-Man_{20})$_{10\%}$ in the presence of mannan as a competitor further confirms the CD206-mediated targeting and internalization of mannosylated liposomes in infected macrophages.

L-(Chol-Man_{20})$_{10\%}$ liposomes delivery of gentamicin to all macrophages, both infected and non-infected subpopulations, might be an important consideration not only for effective exposure to encapsulated antibiotic of intracellular *Salmonella* and their killing, but also in a wider context of in vivo dynamics of *Salmonella* infection; this is dominated by immediate internalization of bacteria released following cell lysis by host phagocytes.[58,59] "Preloading" with gentamicin of non-infected macrophages may make these cells non-permissive to infection, halting the bacterial spread and, potentially, bypassing persistence—since the released bacteria are in a replicative state (as they derive from growing intracellular populations).

2.4. In Vivo Targeting of Macrophages

To demonstrate targeting potential of mannosylated liposomes in the more complex in vivo milieu, we employed transgenic zebrafish embryos which express mCherry fluorescent protein in macrophages (mpeg1-mCherry).[60] Zebrafish embryos are transparent, which enabled us to directly visualize fluorescence colocalization of injected liposomes and macrophages in situ in a living embryo. L-Chol or L-(Chol-Man_{20})$_{10\%}$ liposomes, fluorescently labeled with DiD, were injected into the hindbrain ventricles (**Figure 4**A), known to be a defined anatomical compartment, and the embryos followed over 18 h (Figure 4B). Visual observation of the images illustrates the presence of liposomes-associated DiD fluorescent foci in the hindbrain ventricles, in addition to diffuse signal (yellow channel for DiD liposomes). Image analysis hence correlated the pixel intensity of the DiD fluorescent probe (liposomes) with fluorescence intensity of mCherry (macrophages). The resultant average Pearson coefficients are in a range between 0.4 and 0.55 for L-Chol, and 0.6 and 0.65 for L-(Chol-Man_{20})$_{10\%}$ injected fish (Figure 4C). A further image analysis (Figure 4D) shows a difference in macrophage-associated fluorescence (arising from DiD) in fish injected with non-targeted L-Chol and mannose-presenting L-(Chol-Man_{20})$_{10\%}$ liposomes in all injected fish during 18 h of monitoring. This difference of non- versus mannose-presenting liposomes points to an enhanced macrophage association of mannosylated liposomes in vivo, in line with in vitro data (Figures 2 and 3).

2.5. In Vitro Treatment of *Salmonella* Infection

In this experiment, gentamicin was incorporated into mannosylated, L-(Chol-Man_{20})$_{10\%}$, and non-mannosylated, L-Chol, liposomes at gentamicin concentration of 18 μg mL^{-1} (Figures S40 and S41, Supporting Information), with average particle diameters of 138 ± 1 and 153 ± 2 nm, respectively, and the formulations tested in an in vitro model of *Salmonella* Typhimurium SL1344 infection of RAW 264.7 macrophages (Figure S42, Supporting Information). *Salmonella* survival data, following different treatment conditions, are shown in **Figure 5**.

Culture of *Salmonella*-infected, non-treated RAW 264.7 cells resulted in 8.97×10^5 CFU mL^{-1}; taken as 100% bacterial survival. Empty (no gentamicin containing) L-Chol, and empty mannose-presenting L-(Chol-Man_{20})$_{10}$ liposomes do not show measurable antibacterial activity. Infected macrophages treated with "free" gentamicin dissolved in the cell culture medium show intracellular infection at 8.76×10^5 CFU mL^{-1} (≈4.4 bacteria per cell), equivalent to 98% bacterial survival. Prior to application of gentamicin-loaded liposomes, we assessed if a significant release of encapsulated gentamicin would occur from liposomes while these are incubated with, and before their internalization by macrophages, as this would substantially reduce the dose delivered intracellularly. We thus incubated gentamicin-loaded liposomes with *Salmonella* culture with the view that if such a release occurs, we would observe a consequent effect of released gentamicin on *Salmonella* growth curve. The experiment shows no impact on the growth curve (Figure S41, Supporting Information). Figure 5 illustrates that treatment with gentamicin-containing liposomes, either L-Chol or mannosylated L-(Chol-Man_{20})$_{10}$ formulations, results in a significant reduction in intracellular *Salmonella* survival: 63.7% (5.71×10^5 CFU mL^{-1}) survival for L-Chol, and 18.3% (1.64×10^5 CFU mL^{-1}) for application of mannosylated L(Chol-Man_{20})$_{10\%}$ liposomes, relative to untreated control and "free" gentamicin. It should be noted that these levels of bacterial killing are obtained following a single application of antibiotic-containing formulations, with a total exposure period of 6 h. The results obtained clearly indicate the role that both delivery as liposomal formulation, and indeed as targeted liposomal formulation, have in increasing exposure of intracellular bacteria to cell membrane-impermeable gentamicin. The data furthermore reflect observed differences in internalization of liposomes by subpopulations of macrophages (Figure 3C): mannosylated L-(Chol-Man_{20})$_{10}$ liposomes are internalized by all macrophages and, importantly, by all infected cells. On the contrary, a subpopulation of ≈42% of infected macrophages does not show association with L-Chol liposomes—potentially translated into 63.7% of *Salmonella* survival observed in Figure 5.

It should be noted that treatment of *Salmonella*-infected macrophages with mannose CD206 receptor competitor (mannan) shows a statistically significant increase in *Salmonella*

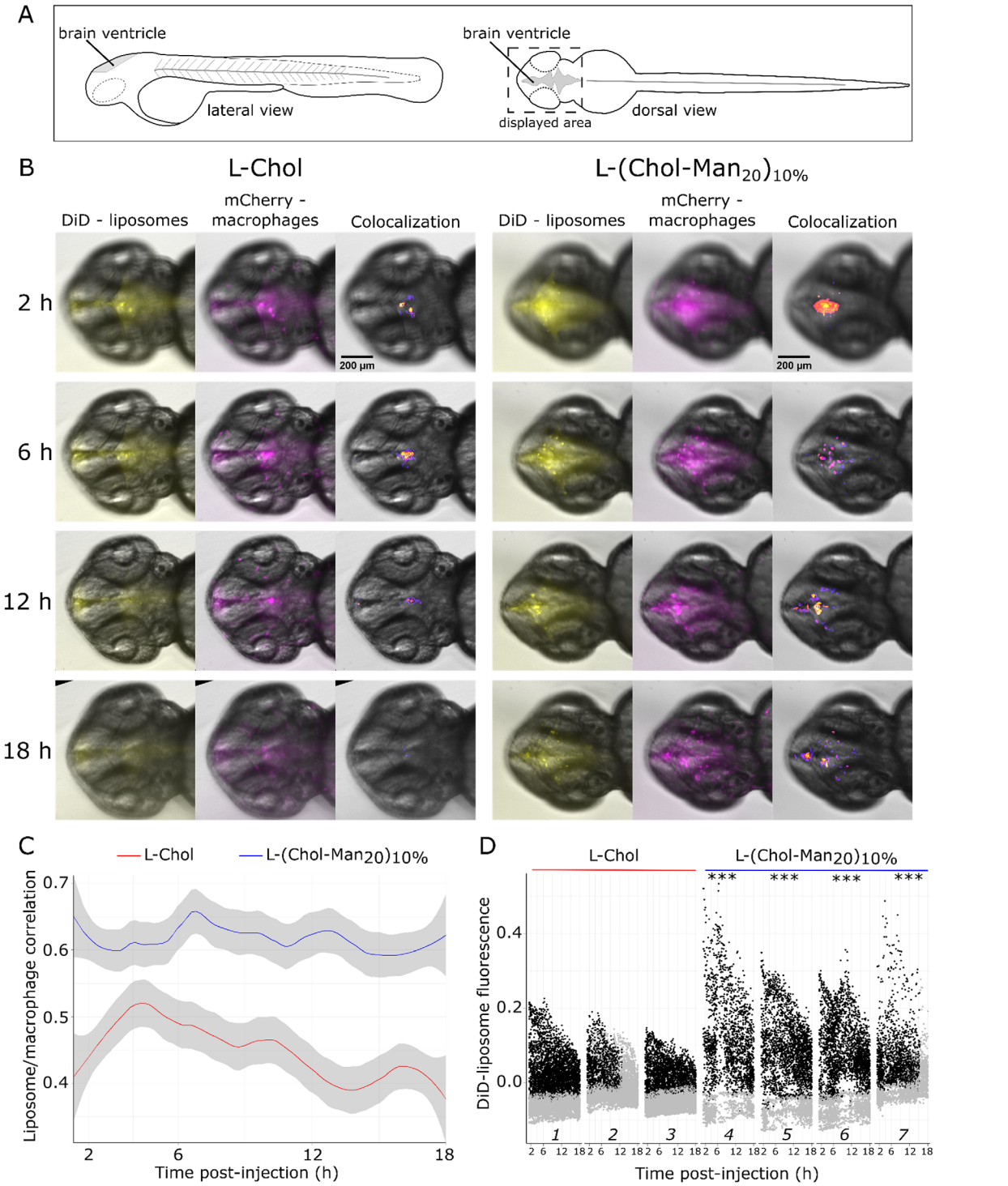

Figure 4. Mannosylated liposomes biodistribution in vivo in zebrafish embryos. A) Schematic representation of fish model and injection site. B) Zebrafish embryos bearing mCherry macrophages (magenta) were injected with DiD-labeled L-Chol or L-(Chol-Man_{20})$_{10\%}$ liposomes (yellow) and imaged by fluorescence microscopy for 18 h. Colocalization of mCherry-macrophages and DiD-liposomes is shown in representative images from individual fish. C) Colocalization analysis of clusters of DiD-fluorescence arising from liposomes, as seen in (B), and mCherry fluorescence of macrophages is shown. The resultant liposome/macrophage average Pearson correlation coefficients of L-Chol and L-(Chol-Man_{20})$_{10\%}$ group of fish versus time are presented. D) Quantification of macrophage associated liposomes from fish injected with L-Chol or L-(Chol-Man_{20})$_{10\%}$ liposomes. Images of injected fish were captured over 18 h and analyzed using an automated pipeline (CellProfiler), as described in Experimental Section. The subtraction applied results in apparently negative fluorescence values for macrophages with no associated DiD, particularly dominant for mCherry-macrophages outside of the hindbrain ventricles (grey dots). For (C) and (D), data were statistically tested compared to the control fish using a Kruskal–Wallis test, followed by pairwise Wilcoxon tests, with a Benjamini–Hochberg correction. *** indicates a $p < 2 \times 10^{-15}$.

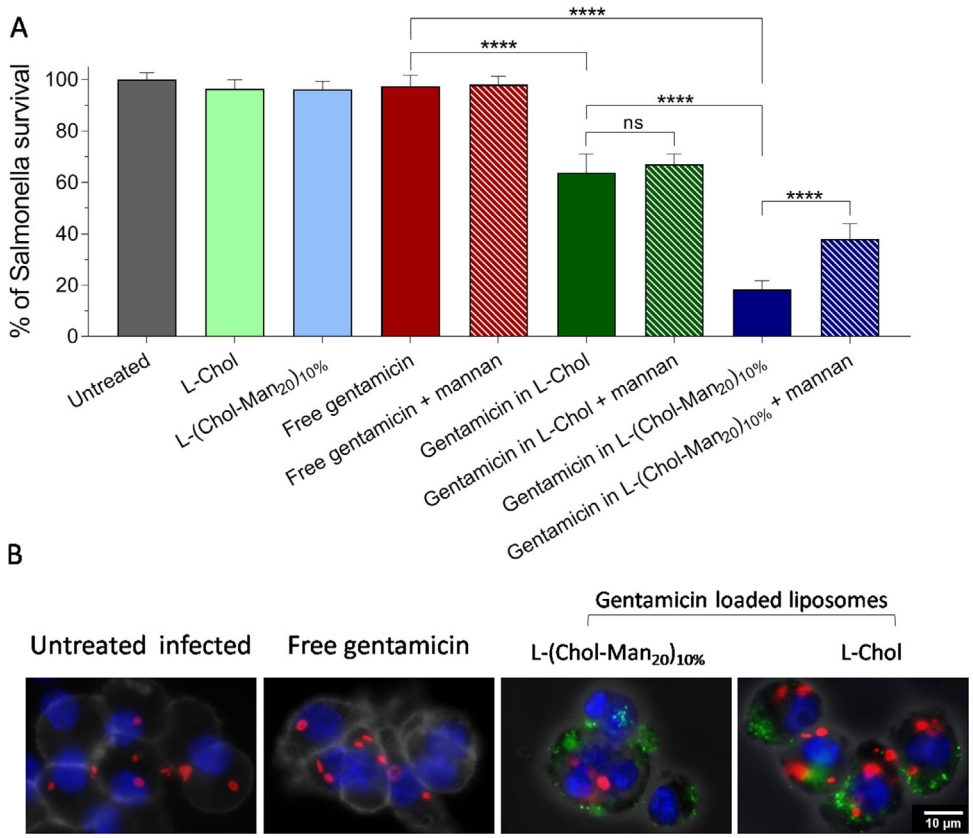

Figure 5. A) Killing of *Salmonella* Typhimurium infection with gentamicin-loaded liposomes. Schematic of the experimental setup, as described in the Experimental Section, is shown in Figure S42, Supporting Information. Infected cells are treated with either "free gentamicin" solution at concentration of 18 µg mL^{-1}, or the equivalent gentamicin concentrations loaded into non-targeted, L-Chol, or targeted mannosylated L-(Chol-Man$_{20}$)$_{10\%}$ liposomes. Bacterial survival is expressed as % of colonies (CFU) relative to *Salmonella* Typhimurium SL1344-infected, untreated RAW 264.7 cells. ****$p < 0.0001$ by one-way ANOVA; "ns" not statistically different. Mannan is used as a competitive ligand for CD206; applied at 1 mg mL^{-1}.[52] $N = 3$ and $n = 3$. B) Representative fluorescence microscopy images; overlay: gray bright field image of cells, blue cell nucleus (DAPI), red SL1344 DsRed2 *Salmonella*, and green liposomes (DiD).

survival for mannosylated L-(Chol-Man$_{20}$)$_{10}$ liposomes, but no significant difference for non-mannosylated L-Chol liposomes. This correlates with the reduction in cellular internalization of mannosylated liposomes seen in the presence of mannan (Figure 3B), and a presence of a subpopulation of ≈56% of infected cells with no liposomes (Figure 3C) on addition of mannan, confirming the critical role of mannose receptor-mediated endocytosis of mannosylated liposomes in eradicating *Salmonella* infection in macrophages.

Models of *Salmonella* infection in vitro and in vivo have shown that a subpopulation of bacteria inside macrophages replicate very slowly, or not at all, for some hours following uptake.[37,61] It is likely that this contributes to a surviving subpopulation of ≈18% of intracellular bacteria seen in this study; similar 20% of antibiotic-refractory *Salmonella* were found in macrophages at 6 h post-infection by others.[62] Future work should address the relationship between dynamics of bacterial replication (as in ref. [37]), and the intracellular drug release from liposomes in relation to a persistence of infection, to optimize a potential therapy regime.

In summary, *Salmonella* killing with gentamicin-loaded liposomes, and with significantly increased efficiency using mannosylated liposomes, suggests that intracellularly delivered gentamicin is "bioavailable," that is, that intracellularly present bacteria are exposed to the antibiotic at killing concentrations. The study hence demonstrates in vivo targeting of macrophages (Figure 4) and eradication of intracellular infection (Figure 5) by the mannosylated liposomes, providing a mechanistic understanding of the system's design, whereby potential advantages and efficacy of the system in a therapy of intracellular infections will need to be assessed in a relevant in vivo model designed to delineate intracellular versus extracellular bacterial killing. This is particularly important as in infection, membrane-impermeable antibiotics act on extracellular bacteria present in extracellular space when high bacterial numbers are reached in the tissues. Hence it would be essential to establish a relevant in vivo model for the purpose of gaining a mechanistic understanding in whether a designed drug delivery system provides a difference in intracellular versus extracellular bacterial killing.

3. Discussion

Our data suggest that mannosylated liposomes are internalized by RAW 264.7 macrophages, in a significant part, via mannose

receptor-driven endocytosis, as clearly demonstrated in experiments with mannan competitor and chlorpromazine inhibition of clathrin endocytosis implicated in mannose receptor internalization pathway (Figure 3B). Furthermore, significant differences are observed in mannosylated liposomes' internalization by subpopulations of macrophages relative to non-mannosylated counterpart (Figure 3C). Notably, liposomes' internalization by RAW 264.7 cells may also occur by other pathways, as illustrated by internalization of L-Chol liposomes, and which are not affected by the presence of mannan (i.e., mannose receptor) or chlorpromazine (i.e., clathrin pathway) (Figure 3B,C), and could contribute to intracellular bioavailability of the antibiotic, as illustrated by reduction in the *Salmonella* survival on treatment with control L-Chol liposomes (Figure 5).

Considering a subpopulation of *Salmonella*-infected cells in more detail, and focusing on the role of CD206 receptor-driven endocytosis, in macrophages mannose receptor can mediate both clathrin-dependent endocytosis of ≈<200 nm material, as well as phagocytosis of larger >500 nm material, including microorganisms, although its function in the latter process is less understood.[30] These internalization processes are mechanistically and functionally distinct. In mannose-mediated endocytosis, from clathrin-coated pits, mannose receptor and its cargo are recruited to early endosomes, from which the receptor recycles to plasma membrane once the cargo is released. This would mean that mannosylated sub-200 nm liposomes, internalized via mannose receptor-driven endocytosis, will, in the absence of endosomolytic functionality, separate from the recycling receptor in the endosome and follow the endocytic pathway toward lysosomal compartments. This poses a question of access of encapsulated gentamicin to intracellularly present *Salmonella*, that is, exposure of membrane-bound *Salmonella* in *Salmonella* Containing Vacuoles (SCV) to intracellularly delivered antibiotic which as "free" is unable to cross lipid bilayer membranes.[57] SCVs had been described as not connected to endocytic pathway;[63] however recent studies demonstrate that connections and intensive dynamic interactions between SCVs and endosomes indeed exist.[64,65] SCVs, however, remain devoid of hydrolytic lysosomal enzymes in their vacuolar membrane that would damage *Salmonella*. It is beyond the scope of this study, and hence we refer to a seminal work by Holden's group[57] which illustrates that SCVs do undergo fusion with lysosomes, but whose "potency" is reduced by bacterial secreted effector protein SifA. This SCV–lysosome interaction could provide an explanation for the exposure of *Salmonella* to the mannosylated liposomes-delivered gentamicin in this study.

Another possible contribution to consider is a release of endocytosed, lysosomally accumulated gentamicin when its concentration in lysosomes exceeds a threshold and potentially, due to its polycationic nature, destabilizes the lysosomal membrane.[66,67] In this scenario, gentamicin would be released into the cytosol and, to access *Salmonella*, would then need to permeate across SCV membrane; the process not likely to occur due to the low membrane permeability of gentamicin. It could be potentially possible that accumulated cytosolic concentration of gentamicin damages the SCV membrane and, in that way, access *Salmonella*. However, such a concentration of cytosolic gentamicin would act on mitochondria and activate the mitochondrial pathway of apoptosis,[68,69] while the rupture of lysosomes would cause the release of proteases into the cytosol, which would induce cell death.[70] We have not observed appreciable macrophage death at the end of our experiment (cells were counted before and after the infection and the treatments, and no significant variations in cell numbers were observed) to support the lysosome destabilization hypothesis.

4. Conclusion

In conclusion, our study describes that surface functionalization, that is, glycosylation of liposomes with oligo-mannose glycolipids, allows efficient receptor-mediated internalization of liposomes-encapsulated antibiotic cargo by *Salmonella*-infected macrophages. Detailed analysis of macrophage subpopulations (Figure 3C) indicates that the superiority of mannosylated liposomes to non-targeted counterparts in killing intracellular bacterial infection is most probably a consequence of internalization of mannosylated liposomes by the entire macrophages population, and indeed infected macrophages subpopulation, driven by mannose-receptor mediated targeting. This represents a crucial consideration for future development of delivery systems for antibiotics aimed at eradication of intracellular infections and offers the potential for future-repurposing of antibacterial agents currently excluded from therapy of intracellular infections due to their low cell membrane permeability.

5. Experimental Section

Synthesis of Membrane-Inserting Mannose Ligands: Detailed descriptions of the materials and methods used in the synthesis of membrane-inserting mannose ligands are provided in Section S1, Supporting Information.

Preparation and Characterization of Liposomes: Liposomes were fabricated by the classical hydration of a thin lipid film method,[71] as detailed in Section S2, Supporting Information. The mean diameter and particle size distribution of liposome formulations were determined by dynamic light scattering (ZetaSizer 2000, Malvern Instruments) at 25 °C using disposable ZEN0040 cuvettes. Results were the mean ± standard deviation (SD) of three repeats.

Concanavalin A Binding Study: ConA lectin binding studies of mannosylated liposomes were performed according to Muller and Schuber's method,[72] as described in Section S2, Supporting Information. A regression line best fit to the aggregation curve for the first 30 s was calculated for each liposome formulation, and the slope used to estimate the initial aggregation rate. The tests were repeated thrice; data reported were the average ± standard deviation.

Mannose Receptor Expression in RAW 264.7 Cells: For analysis of cell surface and total expression of the CD206 receptor, RAW 264.7 were cultured in DMEM medium with or without interleukin IL-4 (Gibco), added at 20 ng mL^{-1} concentration for 48 h. The cells (10^5 cells/100 µL) were blocked with anti-mouse CD16/CD32 antibody (BD Biosciences) to reduce non-specific receptor binding and subsequently incubated with primary antibody Alexa Fluor 647-conjugated anti-mouse MMR/CD206 or isotype control (BioLegend). Antibody incubation was conducted according to the supplier's protocol. Alexa Fluor 647-conjugated anti-mouse CD206 antibody was added at 100 ng mL^{-1}. Flow cytometry was performed on MoFlo Astrios Cell sorter (Beckman Coulter) and analyzed using Weasel Software version 3.5 as described in Section S3, Supporting Information.

RAW 264.7 Cells Internalization of Liposomes and Infection Studies: RAW 264.7 cells, with or without IL-4 treatment, were seeded at a density of 2×10^4 cells/100 µL in a black 96-well plate and incubated at 37 °C in 0.1 mL of growth DMEM medium. For *Salmonella* infection, *Salmonella*

Typhimurium SL1344 expressing a DsRed2 fluorescence[73] was used, as described in Section S6 and Figure S42, Supporting Information. 0.1 mL of the selected liposomal formulations (at 1.0 mM of total lipid concentration in HEPES-buffered HBSS) was applied. The cells were incubated for 2 h at 37 °C. After this time, the liposomal suspension was removed, and cells were washed thrice with PBS and lysed with DMSO (0.1 mL/well). Cellular internalization of liposomes was assessed by measuring the intensity of DiD fluorescence in cell lysates (Tecan Plate Reader, λ_{ex} = 610 nm and λ_{em} = 670 nm). For CD206 receptor competitor experiments, IL-4-treated cells were incubated with chlorpromazine (10 μg mL^{-1}) or mannan (1 mg mL^{-1}—mannan from *Saccharomyces cerevisiae*, Sigma-Aldrich) for 30 min prior to the addition of tested samples. Data represented the mean (±SD) of three independent experiments (N = 3 and n = 5). For flow cytometry measurements, cells were seeded in 12-well plates at a density of 10^5 cells/mL. After infection with *Salmonella* Typhimurium SL1344, expressing a DsRed2 fluorescence, and incubation with liposomes (as above), the cells were washed with PBS and detached from the plates by 5 min incubation at 37 °C with Accutase (Sigma-Aldrich) following supplier's protocol. Cell suspension obtained was centrifuged, fixed with 4% formaldehyde, washed with glycine buffer (0.1 mM in PBS), and resuspended in PBS. DiD and DsRed2 fluorescence was acquired by FACS using a MoFlo Astrios Cell sorter Beckman Coulter; 10^4 events/sample were acquired and analyzed using Weasel Software version 3.5. Data represented the mean (±SD) of three independent experiments. Gating strategy is illustrated in Figure S38, Supporting Information.

Zebrafish Embryo Study: Zebrafish embryo experiments were performed in accordance with the UK Animals (Scientific Procedures) Act 1986 legislation and breeding and maintenance was carried out under Home Office Project Licence number 30/3378. Tg(*mpeg1*:Gal4-FF)gl25/Tg(UAS-E1b:nfsB.mCherry)c264 transgenic zebra fish embryos were raised in E2 buffer at 28 °C, supplemented with 0.003% 1-phenyl-2-thiourea (Sigma-Aldrich) from 24 h post-fertilization to prevent melanin formation. At 48 h post-fertilization, larvae were dechorionated and then anaesthetized with 200 μg mL^{-1} Tricaine (Sigma-Aldrich). Fluorescently labeled liposomes were injected into the hindbrain ventricle (1 nL of 10 mM total lipids in HEPES-buffered HBSS). Larvae were then embedded in low melting point agarose (1.5% in E2 buffer) and supplemented with 0.003% 1-phenyl-2-thiourea and 200 μg mL^{-1} Tricaine. Imaging was performed using a Leica M205FA fluorescence stereomicroscope. Images were collected as z-stacks of ten planes over 486 microns, every 10 min for 144 time points, starting 120 min after injection of liposomes (following embedding in agarose procedure). In-focus slices from Z-stacks at each time point were then automatically selected using an ImageJ macro[74] and analyzed using CellProfiler 3.1.8. The image analysis performed is detailed in Section S4, Supporting Information.

Salmonella Killing Study: The concentration of gentamicin encapsulated into liposomes used in this experiment was determined by agar diffusion assay (Section S5 and Figure S41, Supporting Information). RAW 264.7 cells were infected with SL1344 DsRed2 *Salmonella* Typhimurium with a multiplicity of infection (MOI) of ten bacteria per cell, as described in Section S6 and Figure S42, Supporting Information.

Supporting Information

Supporting Information is available from the Wiley Online Library or from the author.

Acknowledgements

This work was supported by the grants from Engineering and Physical Sciences Council (grant numbers: EP/I01375X/1, EP/N50970X/1). The authors wish to thank Prof. E Sockett and Dr. M Gering for providing access to microscopy and zebrafish resources used, and to the Flow Cytometry Facility team (Dr. D. Onion and N. Croxall) at School of Life Sciences, University of Nottingham.

Conflict of Interest

The authors declare no conflict of interest.

Data Availability Statement

The data that support the findings of this study are available in https://doi.org/10.7910/DVN/CXW9TI.

Keywords

antibiotic delivery, controlled radical polymerization, intracellular infection, mannose receptors, targeted liposomes

Received: August 3, 2021
Revised: September 9, 2021
Published online: September 24, 2021

[1] S. E. Majowicz, J. Musto, E. Scallan, F. J. Angulo, M. Kirk, S. J. O'Brien, T. F. Jones, A. Fazil, R. M. Hoekstra, *Clin. Infect. Dis.* **2010**, *50*, 882.
[2] R. Balasubramanian, J. Im, J.-S. Lee, H. J. Jeon, O. D. Mogeni, J. H. Kim, R. Rakotozandrindrainy, S. Baker, F. Marks, *Hum. Vaccines Immunother.* **2019**, *15*, 1421.
[3] G. M. Jensen, D. F. Hodgson, *Adv. Drug Delivery Rev.* **2020**, *154*, 2.
[4] P. Lutwyche, C. Cordeiro, D. J. Wiseman, M. St-Louis, M. Uh, M. J. Hope, M. S. Webb, B. B. Finlay, *Antimicrob. Agents Chemother.* **1998**, *42*, 2511.
[5] H. Pinto-Alphandary, A. Andremont, P. Couvreur, *Int. J. Antimicrob. Agents* **2000**, *13*, 155.
[6] C. S. Smillie, M. B. Smith, J. Friedman, O. X. Cordero, L. A. David, E. J. Alm, *Nature* **2011**, *480*, 241.
[7] F. B. Tamburini, T. M. Andermann, E. Tkachenko, F. Senchyna, N. Banaei, A. S. Bhatt, *Nat. Med.* **2018**, *24*, 1809.
[8] Y. Litvak, K. K. Z. Mon, H. Nguyen, G. Chanthavixay, M. Liou, E. M. Velazquez, L. Kutter, M. A. Alcantara, M. X. Byndloss, C. R. Tiffany, G. T. Walker, F. Faber, Y. Zhu, D. N. Bronner, A. J. Byndloss, R. M. Tsolis, H. Zhou, A. J. Bäumler, *Cell Host Microbe* **2019**, *25*, 128.
[9] M. T. Sorbara, K. Dubin, E. R. Littmann, T. U. Moody, E. Fontana, R. Seok, I. M. Leiner, Y. Taur, J. U. Peled, M. R. M. van den Brink, Y. Litvak, A. J. Bäumler, J.-L. L. Chaubard, A. J. Pickard, J. R. Cross, E. G. Pamer, *J. Exp. Med.* **2018**, *216*, 84.
[10] P. Scodeller, L. Simón-gracia, S. Kopanchuk, A. Tobi, K. Kilk, P. Säälik, K. Kurm, M. L. Squadrito, V. R. Kotamraju, A. Rinken, M. De Palma, E. Ruoslahti, T. Teesalu, *Sci. Rep.* **2017**, *7*, 14655.
[11] M. Glaffig, N. Stergiou, S. Hartmann, E. Schmitt, H. Kinz, *ChemMedChem* **2018**, *13*, 25.
[12] J. M. Jaynes, R. Sable, M. Ronzetti, W. Bautista, Z. Knotts, A. Abisoye-ogunniyan, D. Li, R. Calvo, M. Dashnyam, A. Singh, T. Guerin, J. White, S. Ravichandran, P. Kumar, K. Talsania, V. Chen, A. Ghebremedhin, B. Karanam, A. B. Salam, R. Amin, T. Odzorig, T. Aiken, V. Nguyen, Y. Bian, J. C. Zarif, A. E. De Groot, M. Mehta, L. Fan, X. Hu, A. Simeonov, Y. Zhao, H. Lopez, S. Kozlov, N. De Val, C. C. Yates, B. Baljinnyam, J. Marugan, U. Rudloff, *Sci. Transl. Med.* **2020**, *12*, eaax6337.
[13] A. K. Azad, M. V. S. Rajaram, L. S. Schlesinger, *J. Cytol. Mol. Biol.* **2014**, *1*, 5.
[14] F.-Y. Su, S. Srinivasan, B. Lee, J. Chen, A. J. Convertine, T. E. West, D. M. Ratner, S. J. Skerrett, P. S. Stayton, *J. Controlled Release* **2018**, *287*, 1.
[15] C. Yang, S. Krishnamurthy, J. Liu, S. Liu, X. Lu, D. J. Coady, W. Cheng, G. De Libero, A. Singhal, J. L. Hedrick, Y. Y. Yang, *Adv. Healthcare Mater.* **2016**, *5*, 1272.

[16] M. A. Phillips, K. L. White, S. Kokkonda, X. Deng, J. White, F. El Mazouni, K. Marsh, D. R. Tomchick, K. Manjalanagara, K. R. Rudra, G. Wirjanata, R. Noviyanti, R. N. Price, J. Marfurt, D. M. Shackleford, F. C. K. Chiu, M. Campbell, M. B. Jimenez-Diaz, S. F. Bazaga, I. Angulo-Barturen, M. S. Martinez, M. Lafuente-Monasterio, W. Kaminsky, K. Silue, A. M. Zeeman, C. Kocken, D. Leroy, B. Blasco, E. Rossignol, T. Rueckle, D. Matthews, J. N. Burrows, D. Waterson, M. J. Palmer, P. K. Rathod, S. A. Charman, *ACS Infect. Dis.* **2016**, *2*, 945.
[17] M. H. Xiong, Y. J. Li, Y. Bao, X. Z. Yang, B. Hu, J. Wang, *Adv. Mater.* **2012**, *24*, 6175.
[18] P. R. Taylor, S. Gordon, L. Martinez-Pomares, *Trends Immunol.* **2005**, *26*, 104.
[19] K. Drickamer, *Nat. Struct. Mol. Biol.* **1995**, *2*, 437.
[20] K. J. Yarema, C. R. Bertozzi, *Genome Biol.* **2001**, *2*, reviews0004.1.
[21] J. J. Lundquist, E. J. Toone, *Chem. Rev.* **2002**, *102*, 555.
[22] L. L. Kiessling, J. C. Grim, *Chem. Soc. Rev.* **2013**, *42*, 4476.
[23] B. Lundberg, *Chem. Phys. Lipids* **1977**, *18*, 212.
[24] F. J. Szoka, *Annu. Rev. Biophys. Bioeng.* **1980**, *9*, 467.
[25] E. C. Woods, N. A. Yee, J. Shen, C. R. Bertozzi, *Angew. Chem., Int. Ed.* **2015**, *54*, 15782.
[26] D. J. Honigfort, M. H. Zhang, S. Verespy, K. Godula, *Faraday Discuss.* **2019**, *219*, 138.
[27] G. Gody, T. Maschmeyer, P. B. Zetterlund, S. Perrier, *Nat. Commun.* **2013**, *4*, 2505.
[28] S. Perrier, P. Takolpuckdee, C. A. Mars, *Macromolecules* **2005**, *38*, 2033.
[29] H. T. McMahon, E. Boucrot, *Nat. Rev. Mol. Cell Biol.* **2011**, *12*, 517.
[30] L. East, C. M. Isacke, *Biochim. Biophys. Acta* **2002**, *1572*, 364.
[31] V. Ladmiral, G. Mantovani, G. J. Clarkson, S. Cauet, J. L. Irwin, D. M. Haddleton, *J. Am. Chem. Soc.* **2006**, *128*, 4823.
[32] C. W. Cairo, J. E. Gestwicki, M. Kanai, L. L. Kiessling, *J. Am. Chem. Soc.* **2002**, *124*, 1615.
[33] J. Chen, H. N. Son, J. J. Hill, S. Srinivasan, F. Y. Su, P. S. Stayton, A. J. Convertine, D. M. Ratner, *Nanomedicine* **2016**, *12*, 2031.
[34] Y. Gou, J. Geng, S. J. Richards, J. Burns, C. R. Becer, D. M. Haddleton, *J. Polym. Sci., Part A: Polym. Chem.* **2013**, *51*, 2588.
[35] T. D. Curtis, L. Gram, G. M. Knudsen, *Front. Microbiol.* **2016**, *7*, 1056.
[36] X. Wang, X. Wang, D. Teng, R. Mao, Y. Hao, N. Yang, Z. Li, J. Wang, *Sci. Rep.* **2018**, *8*, 4204.
[37] S. Helaine, J. A. Thompson, K. G. Watson, M. Liu, C. Boyle, D. W. Holden, *Proc. Natl. Acad. Sci. USA* **2010**, *107*, 3746.
[38] B. Walloschke, H. Fuhrmann, J. Schumann, *Cell. Immunol.* **2010**, *262*, 58.
[39] D. J. Vigerust, S. Vick, V. L. Shepherd, *BMC Immunol.* **2012**, *13*, 51.
[40] M. J. Davis, T. M. Tsang, Y. Qiu, J. K. Dayrit, J. B. Freij, G. B. Huffnagle, A. Olszewski, *mBio* **2013**, *4*, e00264.
[41] X. He, X. Li, Y. Yin, R. Wu, X. Xu, F. Chen, *J. Cell. Mol. Med.* **2018**, *22*, 1302.
[42] L. Martinez-Pomares, *J. Leukocyte Biol.* **2012**, *92*, 1177.
[43] T. Wileman, R. L. Boshans, P. Schlesinger, P. Stahl, *Biochem. J.* **1984**, *220*, 665.
[44] D. A. C. Stapels, P. W. S. Hill, A. J. Westermann, R. A. Fisher, T. L. Thurston, A. E. Saliba, I. Blommestein, J. Vogel, S. Helaine, *Science* **2018**, *362*, 1156.
[45] M. Orecchioni, Y. Ghosheh, A. B. Pramod, K. Ley, *Front. Immunol.* **2019**, *10*, 1084.
[46] A. Engel, S. K. Chatterjee, A. Al-arifi, D. Riemann, J. Langner, P. Nuhn, *Pharm. Res.* **2003**, *20*, 51.
[47] A. Engel, S. K. Chatterjee, A. Al-Arifi, P. Nuhn, *J. Pharm. Sci.* **2003**, *92*, 2229.
[48] J. Senior, G. Gregoriadis, *Life Sci.* **1982**, *30*, 2123.
[49] A. V. Samsonov, I. Mihalyov, F. S. Cohen, *Biophys. J.* **2001**, *81*, 1486.
[50] T. Baumgart, S. T. Hess, W. W. Webb, *Nature* **2003**, *425*, 821.
[51] J. H. Risselada, S. J. Marrink, *Proc. Natl. Acad. Sci. USA* **2008**, *105*, 17367.
[52] S. Dasgupta, A. M. Navarrete, J. Bayry, S. Delignat, B. Wootla, S. André, O. Christophe, M. Nascimbeni, M. Jacquemin, L. Martinez-Pomares, T. B. H. Geijtenbeek, A. Moris, J. M. Saint-Remy, M. D. Kazatchkine, S. V. Kaveri, S. Lacroix-Desmazes, *Proc. Natl. Acad. Sci. USA* **2007**, *104*, 8965.
[53] P. G. Royall, D. Q. Craig, C. Doherty, *Int. J. Pharm.* **1999**, *192*, 39.
[54] A. Alshehri, A. Grabowska, S. Stolnik, *Sci. Rep.* **2018**, *8*, 3748.
[55] F.-Y. Su, J. Chen, H.-N. Son, A. M. Kelly, A. J. Convertine, D. M. Ratner, P. S. Stayton, *Biomater. Sci.* **2018**, *6*, 1976.
[56] S. Stolnik, L. Illum, S. S. Davis, *Adv. Drug Delivery Rev.* **2012**, *64*, 290.
[57] D. W. Holden, *Traffic* **2002**, *3*, 161.
[58] S. P. Brown, S. J. Cornell, M. Sheppard, A. J. Grant, D. J. Maskell, B. T. Grenfell, P. Mastroeni, *PLoS Biol.* **2006**, *4*, e349.
[59] A. J. Grant, O. Restif, T. J. McKinley, M. Sheppard, D. J. Maskell, P. Mastroeni, *PLoS Biol.* **2008**, *6*, e74.
[60] F. Ellett, L. Pase, J. W. Hayman, A. Andrianopoulos, G. J. Lieschke, *Blood* **2011**, *117*, e49.
[61] S. Helaine, A. M. Cheverton, K. G. Watson, L. M. Faure, S. A. Matthews, D. W. Holden, *Science* **2014**, *343*, 204.
[62] A. Claudi, P. Spröte, A. Chirkova, N. Personnic, J. Zankl, N. Schürmann, A. Schmidt, D. Bumann, *Cell* **2014**, *158*, 722.
[63] M. Rathman, L. P. Barker, S. Falkow, *Infect. Immun.* **1997**, *65*, 1475.
[64] K. Mukherjee, S. A. Siddiqi, S. Hashim, M. Raje, S. K. Basu, A. Mukhopadhyay, *J. Cell Biol.* **2000**, *148*, 741.
[65] K. Mcgourty, T. L. Thurston, S. A. Matthews, L. Pinaud, L. J. Mota, D. W. Holden, *Science* **2012**, *338*, 963.
[66] E. O. Ngaha, I. O. Ogunleye, *Biochem. Pharmacol.* **1983**, *32*, 2659.
[67] A. L. Regec, B. F. Trump, A. L. Trifilis, *Biochem. Pharmacol.* **1989**, *38*, 2527.
[68] A. I. Morales, D. Detaille, M. Prieto, A. Puente, E. Briones, M. Arévalo, X. Leverve, J. M. López-Novoa, M. Y. El-Mir, *Kidney Int.* **2010**, *77*, 861.
[69] C. F. Simmons, R. T. J. Bogusky, D. H. Humes, *J. Pharmacol. Exp. Ther.* **1980**, *214*, 709.
[70] R. G. Schnellmann, S. W. Williams, *Renal Failure* **1998**, *20*, 679.
[71] A. D. Bangham, M. M. Standish, J. C. Watkins, *J. Mol. Biol.* **1965**, *13*, 238.
[72] C. D. Muller, F. Schuber, *Biochim. Biophys. Acta, Biomembr.* **1989**, *986*, 97.
[73] A. Huett, A. Ng, Z. Cao, P. Kuballa, M. Komatsu, M. J. Daly, D. K. Podolsky, R. J. Xavier, *J. Immunol.* **2009**, *182*, 4917.
[74] Y. Sun, S. Duthaler, B. J. Nelson, *Microsc. Res. Tech.* **2004**, *65*, 139.